


## Article

# Study on the Liquefaction Mechanism of Mixed-Size Tailings Material Based on Grain Contact State Theory

Chunlin Jiang <sup>1</sup> , Guangjin Wang <sup>1,2,\*</sup>, Yanbo Zhang <sup>3</sup> and Jinglong Liang <sup>4</sup>

<sup>1</sup> Faculty of Land Resources Engineering, Kunming University of Science and Technology, Kunming 650093, China

<sup>2</sup> Yunnan International Technology Transfer Center for Mineral Resources Development and Solid Waste Resource Utilization, Kunming 650093, China

<sup>3</sup> College of Mining Engineering, North China University of Science and Technology, Tangshan 063009, China

<sup>4</sup> College of Metallurgy and Energy, North China University of Science and Technology, Tangshan 063009, China

\* Correspondence: wangguangjin2005@163.com

**Abstract:** Tailings ponds serve as high-potential energy structures designed to store waste tailings and other industrial materials. However, they can give rise to significant environmental pollution and pose a substantial threat to social and economic development, as well as the safety of people's lives and property. Seismic disasters can cause liquefaction of tailings, leading to destabilization and dam failure of tailings ponds, and the evolution of dynamic pore pressure of tailings can indirectly reflect the destabilization process of tailings ponds. Fine grain content is one of the main factors affecting the dynamic strength and pore pressure development of tailings. This article studies the microscopic characteristics of tailings material through microscopic observation, triaxial testing, discrete element simulation, and grain contact state theory, aiming to analyze the influence mechanism of fine grain content on the micromechanics of tailings. Based on the grain contact state theory, the tailings with different fine grain contents are classified into three types: coarse grain tailings, intermediate-size grain tailings, and fine grain tailings, and the grain contact is classified into four different states. In contact state 1, the vibration pore pressure exhibits a "fast-stable" development mode with increasing vibrations. In contact state 2 or 3, the vibration pore pressure develops linearly with vibrations. For contact state 4, the development of vibration pore pressure presents a "fast-stable-sharp" development mode. The effect of fine grain content ( $FC$ ) on the liquefaction of the tailings studied in the present work is as follows. When the fine grain content is  $FC < 30\%$ , the liquefaction resistance of the tailings decreases with the increase of  $FC$ . When  $FC > 30\%$ , the liquefaction resistance increases with the increase of  $FC$ . When  $FC = 30\%$ , the liquefaction resistance is the lowest, indicating that the critical threshold of the fine grain content of the tailings studied in the present work is  $FC_{th} = 30\%$ .

**Keywords:** grain contact state; fine grain content; tailings material; microscopic observation; discrete element simulation (PFC3D)



**Citation:** Jiang, C.; Wang, G.; Zhang, Y.; Liang, J. Study on the Liquefaction Mechanism of Mixed-Size Tailings Material Based on Grain Contact State Theory. *Buildings* **2023**, *13*, 1808. <https://doi.org/10.3390/buildings13071808>

Academic Editors: Qingbiao Wang and Bin Gong

Received: 25 May 2023

Revised: 3 July 2023

Accepted: 13 July 2023

Published: 16 July 2023



**Copyright:** © 2023 by the authors. Licensee MDPI, Basel, Switzerland. This article is an open access article distributed under the terms and conditions of the Creative Commons Attribution (CC BY) license (<https://creativecommons.org/licenses/by/4.0/>).

## 1. Introduction

In China, tailings ponds are mostly constructed using upstream dams. In such tailings ponds, the grains of the tailings are relatively fine, leading to noticeable variations in the spatial distribution of grain composition. Consequently, there are significant disparities in the mechanical properties and permeability coefficient of the tailings material [1]. Therefore, applying prior knowledge derived from conventional sand and soil research to tailings engineering can inadvertently result in issues such as overly risky or excessively conservative designs. Hence, it holds paramount theoretical significance and practical value to investigate the impact of fine grain content on the mechanical properties of tailings.

Generally, the content of fine grains significantly impacts the dynamic strength and pore pressure development of soil and sand [2]. At present, the influence of fine grain

content on the strength characteristics of sand has attracted global attention from both academic and engineering communities. Many researchers have studied the matter at various depths, recognizing its significance and relevance in their studies. Seed et al. [3] discovered that the soil liquefaction resistance strength demonstrated an increase in correlation with the rise in fine grain content, while utilizing identical normalized SPT (Standard Penetration Test) strokes. Vaid et al. [4] found that the increase in fine grain content reduced the anti-liquefaction ability of saturated sandy soil, which was completely contrary to the findings of Amini et al. [5] and Monkul et al. [6]. According to Polito et al. [7], for a given void ratio, the anti-liquefaction capacity of fine-grained sand decreased first and then increased with the increase of fine grain content, with the lowest anti-liquefaction strength appearing when the fine grain content was in the range 37~50%. Xenaki et al. [8] pointed out that for a given void ratio, the fine grain content that led to the lowest saturated soil anti-liquefaction strength was 44%. Wand et al. [9] conducted tests on sand with a fine grain content of 0 to 40%, and the results showed that the liquefaction resistance of the sand was the lowest when the fine grain content was 33%. Phan et al. [10] conducted a consolidated undrained triaxial test on sand-silt mixed soil with a fine grain content ranging from 0% to 60% and found that the soil strength first decreased and then increased, with the lowest soil strength appearing when the content was 50%. Lv [11] found that the critical point of dynamic characteristics change of silt was when the fine grain content was in the range of 40~70%, accompanied by a clay content of 12%. Cao et al. [12] found through vibrating triaxial tests that the effect of clay content on the dynamic strength of silt was not monotonous, and the soil sample was most likely to be damaged when the clay content was 9%. Similar findings have been reported by Liu et al. [13], who conducted liquefaction tests on Nanjing silty fine sand with three clay contents and found that the liquefaction resistance did not change monotonically with the increase of clay content, with the liquefaction resistance being the lowest when the clay content was about 10%. Zhou et al. [14], Liu et al. [15], Ruan et al. [16] and others conducted cyclic loading tests on saturated sand with different fine grain contents and achieved many research results [17–23], which further proved the existence of the critical content. Besides the dynamic strength change of sand/soil due to grain content variation, scholars have also focused on studies of the effect of fine grain content on the dynamic pore pressure of saturated silt [24–26]. For instance, Zhao et al. [27] analyzed the influence of clay and silt content on pore pressure development mode based on traditional methods and energy analysis methods. Zeng and Liu [28–31] and Wang et al. [32] conducted many cyclic loading tests on saturated silt with different silt contents to study the impact of silt content on the development of saturated silt vibration pore pressure. Hasan Eker et al. [33] reached the conclusion that substituting volcanic ash material for silicate cement enhanced the strength of paste backfill mixtures at specific cement ratios. Furthermore, it was determined that incorporating volcanic ash in the cemented paste backfill (CPB) improved the mixture's durability against sulfate attack. Deniz Adiguzel et al. [34] conducted a thorough examination of the influence of grain size distribution on the rheological behavior of tailings. Additionally, they proposed a method to effectively manage the impact of variations in grain size distribution on the pumpability of the slurry. Qian Bi et al. [35] concluded that the effect of fine grain content on the stability of tailings dams could not be described by a simplistic function. Cui Minjuan et al. [36] concluded that, in microbially cured sandy soils, calcium carbonate crystals accumulated as grain clusters on the surface of sandy soil grains and at interparticle contacts. The size of these clusters increased with the degree of stacking of calcium carbonate crystals. In sandy soils with smaller grain sizes, the interparticle pores are more readily filled and compacted by calcium carbonate crystals. Consequently, the cured specimens exhibited a larger proportion of effective calcium carbonate crystals, resulting in a stronger structure and higher lateral compressive strength. Wang Y et al. [37] reached the conclusion that the dynamic modulus of elasticity of sandy soil exhibited a decrease as the fine grain content increased. However, this trend reversed when the fine grain content surpassed 30%. Similarly, the damping ratio demonstrated an increasing trend followed by a subsequent decrease with

an increase in fine grain content, with the critical content also being 30%. Notably, these research results were attained mainly through fittings of pore pressure test results.

In general, both domestic and foreign experiments predominantly employ fine sand with specific grain sizes to investigate the impact of fine grain content on the mechanical properties of soil. Moreover, they primarily focus on the dynamic strength characteristics of soil, resulting in limited reporting on the effects of fine grain content on the mechanical properties of tailings material. This study, however, adopts the grain contact state theory as a foundation. It integrates microscopic observation experiments, cyclic dynamic triaxial tests, and discrete element simulations to examine the dynamic pore pressure and dynamic strength characteristics of on-site tailings material with varying fine grain contents. The objective is to obtain a comprehensive understanding of how fine grain content influences the engineering properties of tailings.

## 2. Theory of Grain Contact State of Mixed-Size (Coarse and Fine) Tailings

In order to describe the influence of fine grain content on the mechanical properties and mechanical response of sand with mixed-size grains, Thevanayagam [38] introduced a classification by dividing the sand grains into two groups: coarse grains and fine grains. This division was based on a grain size threshold of 74  $\mu\text{m}$ . The author introduced the concept of grain contact state, where the mechanical properties of the mixed-size sand are determined by the contact state between the coarse and fine grains.

The change in grain contact state affects the microstructure of tailings composed of coarse and fine grains, which can lead to changes in the basic physical properties, shear characteristics and circulation characteristics of the tailings. For mixed-size tailings, there exists a critical threshold of fine grain content, denoted as  $FC_{th}$ . If  $FC < FC_{th}$ ; the structure of the tailings is mainly constructed by coarse grains, otherwise, the structure is mainly built on fine grains. With the increase of  $FC$ , the grain contact state of the mixed-size tailings varies across four types, as shown in Figure 1:

- (1) Contact state 1: Coarse grains are in direct contact, fine grains completely fill the pores between coarse grains, the structure of the tailings is completely composed of coarse grains, and the mechanical properties of mixed-size tailings are completely determined by the coarse grain fabric, as shown in Figure 1a;
- (2) Contact state 2: A small number of fine grains participate in the contact between coarse grains, and most of the fine grains fill the coarse grain pores. The structure of the tailings is composed of coarse grains and a small number of fine grains. The mechanical properties of the tailings are mainly determined by the coarse grain fabric, which has an impact on the mechanical properties of the tailings, as shown in Figure 1b;
- (3) Contact state 3: Most of the fine grains participate in the contact between coarse grains, and a small number of fine grains fill the pores between coarse grains. The structure of the tailings consists of fine grains and a small number of coarse grains. The mechanical properties of the tailings are mainly determined by the fine grains, but the coarse grains still have an impact on the mechanical properties, as shown in Figure 1c;
- (4) Contact state 4: The coarse grains have no direct contact, and the contact between fine grains is independent of the coarse grains. The structure of the tailings is completely composed of fine grains, and the mechanical properties of the mixed-size tailings are completely determined by the fine grain fabric, as shown in Figure 1d.

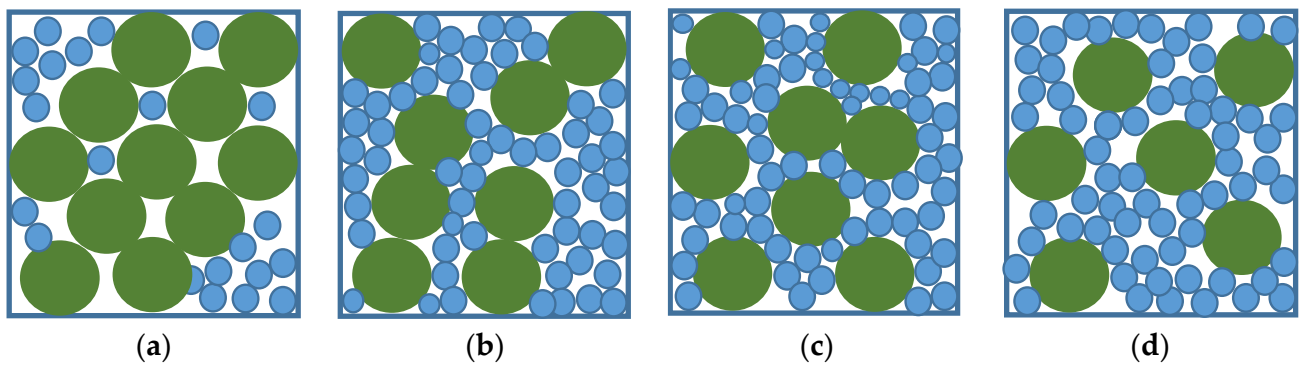


**Figure 1.** Schematic diagrams that demonstrate the four contact states of mixed-size tailings (a–d).

### 3. Undrained Cyclic Dynamic Triaxial Test

#### 3.1. Experimental Instruments and Material

In this experiment, KTL-DYN10 dynamic triaxial equipment, as shown in Figure 2, was selected. The hardware system included an axial loading device, a dynamic confining pressure control room, a back pressure controller, and an 8-channel high-speed control and acquisition device. The software system was a DSP high-speed digital control system with a maximum operating frequency of 10 Hz and a maximum dynamic stress amplitude of  $\pm 10$  kN.



**Figure 2.** KTL-DYN10 dynamic triaxial equipment.

The test samples used in this work were taken from an iron tailings dam in Sichuan, and the raw material was the main construction material for the dam. According to the “Geotechnical Test Code: GBT 50123-2019” [39], it is necessary to presort the coarse and fine grains before preparing the samples. The specific screening method was to use 1 mm and 0.074 mm sieves to screen the soil samples, which had been dried at 110 °C. After the screening, grains whose sizes were in the range of 0.074 mm to 1 mm were defined as coarse grains, and those smaller than 0.074 mm were defined as fine grains. This test used cylindrical samples with a diameter of 50 mm and a height of 105 mm, which were compacted in four layers. After consolidation, the dry density  $\rho_d$  of the samples was controlled at around 1.68 g/cm<sup>3</sup>. Figure 3 shows the grading results of coarse and fine sand grains.

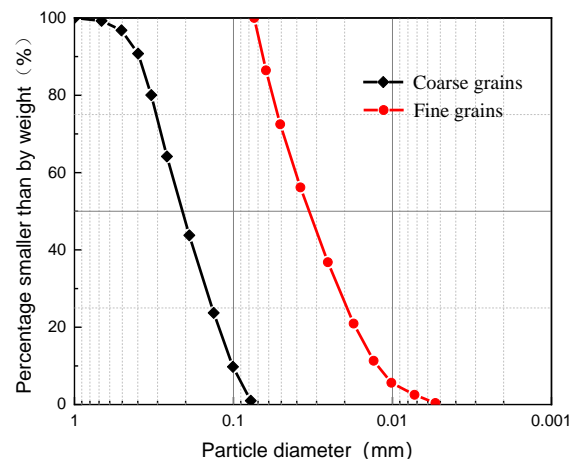


**Figure 3.** Coarse and fine grain size distribution curves.

### 3.2. Experiment Procedure and Scheme

After the samples were prepared, a back-pressure controller was first used to detect their air tightness, and then CO<sub>2</sub> saturation, water head saturation, and back-pressure saturation methods were adopted to increase their saturation to 98% ( $B > 0.98$ ). These tests were conducted under undrained conditions using a stress amplitude cyclic loading method with a test frequency of 1 Hz. Three dynamic stresses ( $\sigma_d$ ) were tested, which were 56, 60, and 64 kPa, and the confining consolidation pressure was fixed at 100 kPa. In the present work, the liquefaction point ( $u = \sigma_3$ ) was adopted as a criterion for terminating the test. More details of the experimental scheme are provided in Table 1.

**Table 1.** Experimental scheme.

Sample No.	Coarse Grain Content	Fine Grain Content	CSR
1 #	100	0	
2 #	90	10	
3 #	80	20	
4 #	70	30	
5 #	60	40	
6 #	50	50	0.28, 0.30, 0.32
7 #	40	60	
8 #	30	70	
9 #	20	80	
10 #	10	90	
11 #	0	100	

Note:  $CSR = \frac{\sigma_d}{2\sigma_3}$ .

## 4. Experimental Results and Discussion

Section 4.1 introduces microscopic observations of the grains by the XRD and SEM tests. XRD tests were used to observe the tailings grain composition, and SEM tests were used to observe the morphology of tailings grains. The pore pressure development pattern of the tailings material with different fine grain contents was investigated. Section 4.2 presents a numerical investigation of the dynamic strength variation of the tailings material due to the change in fine grain content, where force chain and inter-grain contact force played important roles.

### 4.1. Influence of Fine Grain Content on Pore Pressure Development of Tailings Material

Figure 4 shows the dynamic pore pressure development processes of tailings material with different fine grain contents. It can be found that when the fine grain content is 10%, the sample vibration pore pressure development consists of two stages, presenting a

'fast-stable' development mode. The first stage is a fast-growth stage, in which the pore pressure rapidly increases within a few vibration cycles. In the second stage, the pore pressure increment gradually slows down and tends to stabilize. When the content of fine grains is 30%, the vibration pore pressure of the sample develops linearly. For the sample with a fine grain content of 100%, the development of pore pressure can be divided into three stages, presenting a 'fast-stable-sharp' development mode. The growth of pore pressure is fast in the initial stage, stable in the mid stage and becomes very sharp in the late stage.

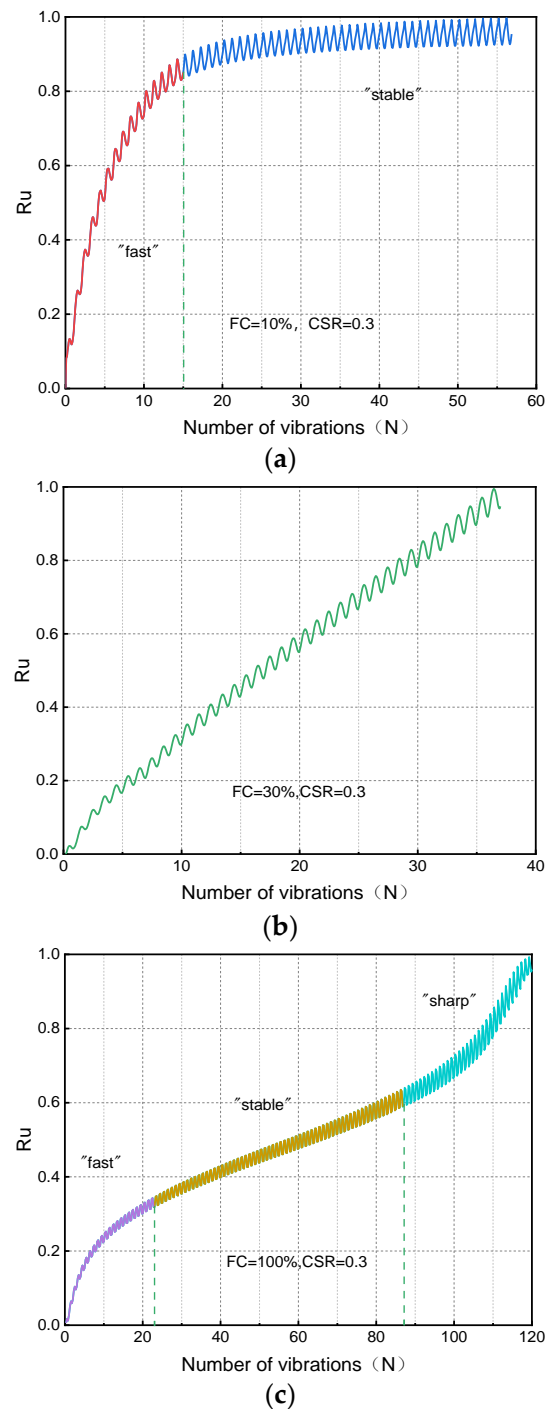


**Figure 4.** Dynamic pore pressure development curves of tailings material with different fine grain contents (a–c).



To explore the microscopic properties of coarse and fine grains, the samples were analyzed using XRD (X-ray Diffraction) testing and SEM testing [40]. The results from various tests can complement and verify each other.

Figures 5 and 6 show the XRD test results and suggest that the tailings material is mainly composed of quartz, illite, chlorite, and dolomite (as well as trace amounts of feldspar, calcite, and metal minerals). As can be seen from the figures, both coarse and fine grains are mainly composed of quartz (non-viscous mineral) and illite (viscous mineral) but with very different component ratios. The content of quartz in the coarse grains is much higher than that of illite, providing the coarse grains with higher hardness and lower viscosity. In the fine grains, the content of quartz decreases, and the content of illite increases, resulting in lower hardness and higher viscosity.

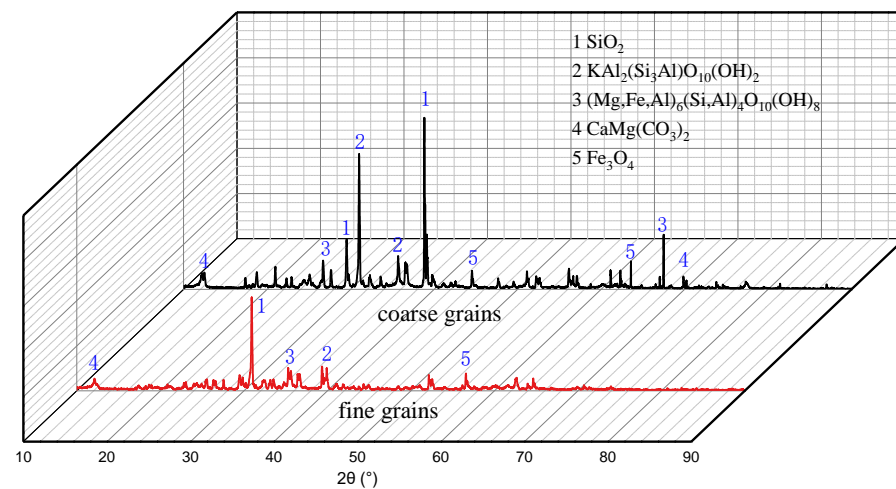


Figure 5. XRD diffraction pattern.

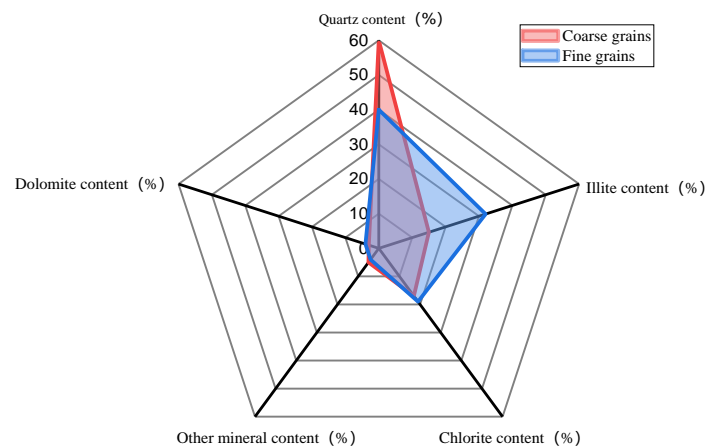
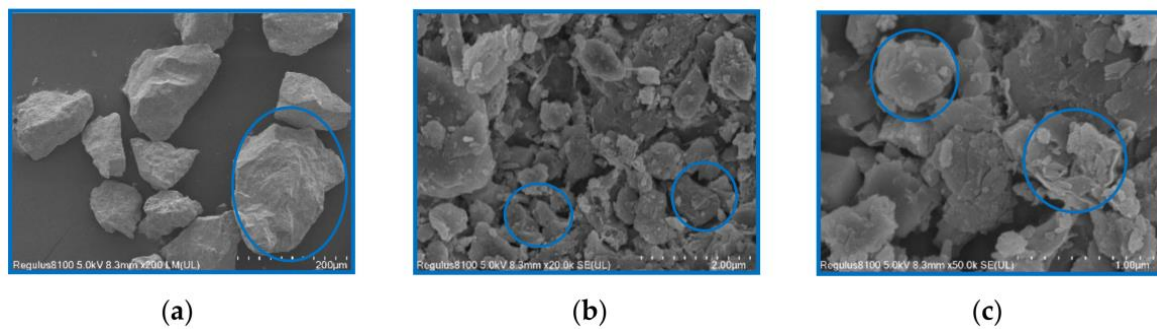
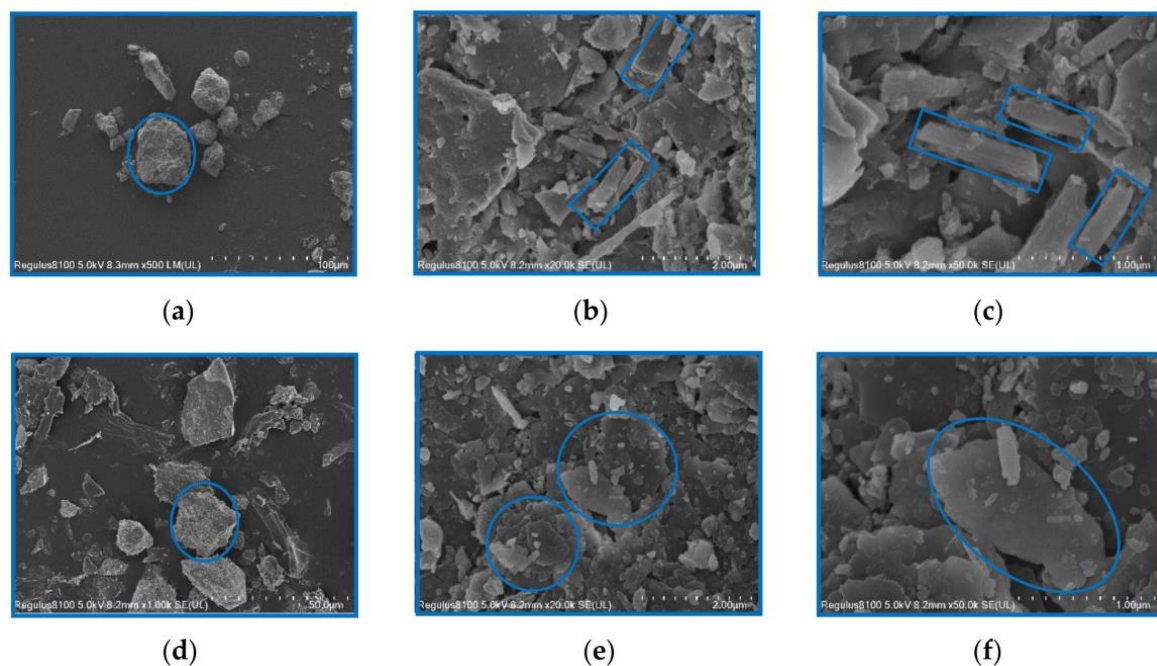


Figure 6. Comparison of compositions of coarse and fine grains.

Figures 7 and 8 present SEM pictures of some coarse and fine grains, respectively. From the analysis results, the coarse grains are all in granular form (Figure 7c), while the fine grains are mainly flakes mixed with little granular grains (Figure 8c,f). In addition, the figures suggest coarse and fine grains are also different in surface morphology and contact form. Coarse grains primarily exhibit edge-to-edge and edge-to-surface contacts (Figure 7b), whereas fine grains predominantly display edge-to-surface and surface-to-surface contacts (Figure 8b,e).



**Figure 7.** Coarse grain shape and surface topography (a–c).



**Figure 8.** Fine grain shape and surface topography (a–f).

The aforementioned phenomena are elaborated as follows. When  $FC = 10\%$ , the grain contact is in state 1, and the tailings are mainly composed of coarse grains, suggesting that the mechanical properties are completely determined by the coarse-grain fabric. Considering that the coarse-grain tailings are mostly granular grains with great hardness and the grains are mostly in edge-to-edge and edge-to-surface contacts, the adhesion between grains is expected to be low. In the initial stage of cyclic loading, the poor structure and low adhesion make the pore water pressure increase rapidly. As the loading progresses, the recombination of grains slows down the growth rate of the pore water pressure.

When  $FC = 30\%$ , the grain contact is in state 2 or 3, and the tailings consist of both coarse and fine grains, which determine the mechanical properties of the sample together. Under the action of cyclic load, some fine grains play a lubricating effect in the pores between coarse grains, weakening the friction force between coarse grains and accelerating the growth rate of pore pressure. At the same time, the other fine grains wrap coarse grains and reduce the growth rate of pore pressure. The combination of the above two mechanisms makes the pore water pressure increase stably throughout the test.

When  $FC = 100\%$ , the grain contact is in state 4, and the tailings are similar to fine-grain sand. The mechanical properties of the sample are completely determined by the fine-grain structure. Since the fine grains are mostly flaky grains with low hardness and exhibit side-to-surface and surface-to-surface contacts, the tailings structure is expected to be weak but with high adhesion. At the beginning of the cyclic loading, the fine grains with



low hardness enable the pore water pressure to increase rapidly. As the loading progresses, the coarse grains are embedded in the viscous fine grains, which slows down the growth rate of the pore water pressure. At the late stage, the recombination of grains speeds up the pore water pressure growth rate again.

#### 4.2. Influence of Fine Grain Content on Dynamic Strength of Tailings Material

The critical threshold of fine grain content, denoted as  $FC_{th}$ , is an important parameter to distinguish the main structure composition of mixed-size tailings. When  $FC < FC_{th}$ , the grain contact of mixed-size tailings is in state 1 or 2. Since fine grains have no or little effect on the mechanical properties of the tailings, coarse grains construct the main tailings structure. The void ratio of the structure is called the intergranular void ratio, denoted using  $e_s$ , and can be obtained by the following formula,

$$e_s = \frac{e + f_c}{1 - f_c} \quad (1)$$

where  $e$  is the total pore volume of the soil,  $f_c$  is the fine grain content (mass percentage number).

When  $FC > FC_{th}$ , the grains of the mixed-size tailings are in contact state 3 or 4. Most or all the coarse grains are surrounded by fine grains and become isolated, resulting in little or no direct contact between coarse grains. Thus, coarse grains have little effect on the mechanical properties of the tailings. In such a case, the fine grains construct the main structure of the tailings, and the inter-fine grain void ratio  $e_f$  is defined as:

$$e_f = \frac{e}{f_c} \quad (2)$$

As shown in Figure 9a, when  $FC < 30\%$ , the grain contact is in state 1 or 2, and the tailings are dominated by coarse grains, which thereby form the main structure of the tailings. The fine grains are unable to fill up all the pores between coarse grains. Therefore, the dynamic characteristics, in this case, are mainly determined by coarse grains. As the content of fine grains increases, the void ratio formed between the coarse grains increases as well, which reduces the direct contact between coarse grains and subsequently weakens the interaction force inside the tailings and the dynamic strength of the tailings.

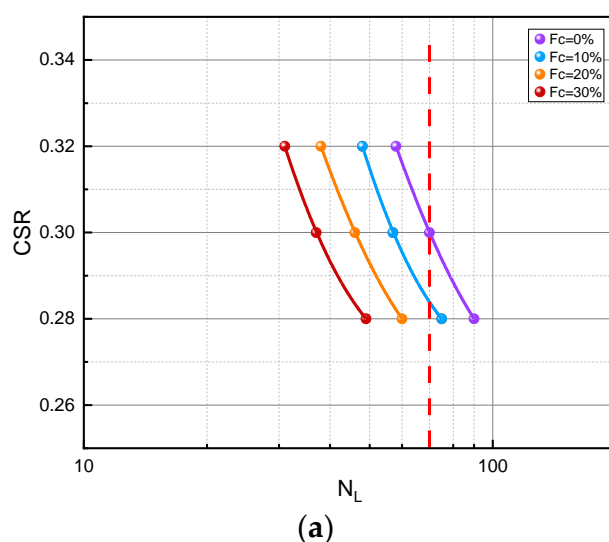
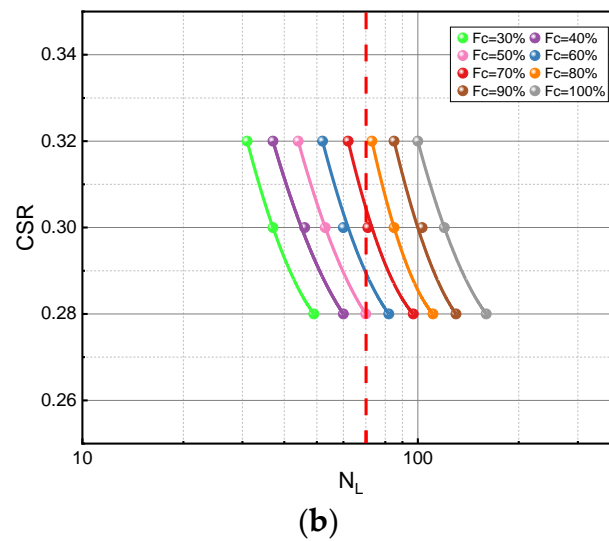


Figure 9. Cont.



**Figure 9.** CSR- $N_L$  curves under different fine grain contents (a,b).

In Figure 9b,  $FC > 30\%$ , the grain contact is in state 3 or 4, and the fine grain content further increases. In such a case, the fine grains not only fill the pores between the coarse grains but also wrap the coarse grains, so the coarse grains are no longer involved in constructing the main structure of the tailings. Thus, the dynamic characteristics of the tailings, in this case, are mainly determined by the fine grains. Since the void ratio between fine grains decreases with the increase of fine grain content, the dynamic strength of the tailings shows an opposite changing trend to that of the case where  $FC$  is less than 30%.

#### 4.3. Micro-Mechanism Analysis

The section studies the micro-mechanism of mixed-size tailings using the discrete element method [41,42]. To verify the rationality of the model parameter selection, Figure 10 compares the stress–strain relationship curve simulated by the PFC static triaxial shear test on a sample with a fine grain content of 30% with that from an indoor triaxial shear test under a confining pressure of 100 kPa [43,44]. Although there is a tiny gap between these two curves, their development patterns are generally consistent, proving the effectiveness of the discrete element model and indicating that the determined contact model parameters in the discrete model are reasonable.

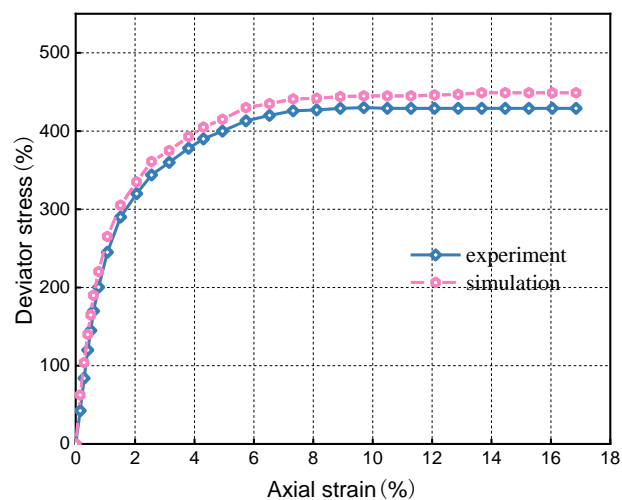


**Figure 10.** Stress–strain curve comparison between simulation and experiment results.

After the model validation, discrete element models with different fine grain contents were established to reproduce the cyclic triaxial loading process of the mixed-sized tailings. The determined coarse and fine grain microscopic parameters and content ratios are listed in Tables 2 and 3.

**Table 2.** Grain parameters in the discrete element model.

Grain Type	Grain Size Range (mm)	Contact Mode	$k_n$ (N/m)	$k_s$ (N/m)	$n\_bond$ (N)	$s\_bond$ (N)	Fric
Coarse	1~0.075	Linear contact	$1 \times 10^8$	$1 \times 10^8$	—	—	0.5
Fine	0.075~0.001	Adhesive contact	$1 \times 10^6$	$5 \times 10^6$	$4 \times 10^3$	$4 \times 10^3$	0.5

**Table 3.** Grain content ratios in the discrete element model.

Sample No.	Coarse Grain Content/%	Fine Grain Content/%
1	90	10
2	80	20
3	70	30
4	50	50
5	30	70

#### 4.3.1. Force Chain Analysis

The influence of fine grain content on the dynamic strength of tailings material can be explained by the microstructure characteristics [45]. The microstructure of tailings is highly intricate, as it encompasses a collection of grains or grain clusters of varying sizes that form through one or more connectivity methods. The different combinations or contact modes between grains are called “force chains” [46,47], which directly affect the macroscopic mechanical state of the tailings.

The density and thickness of the force chains represent the contact status and contact strength between grains and can thereby reflect the main structure of the tailings. The force chain distributions of the DEM samples with different fine grain contents after the consolidation is shown in Figure 11.

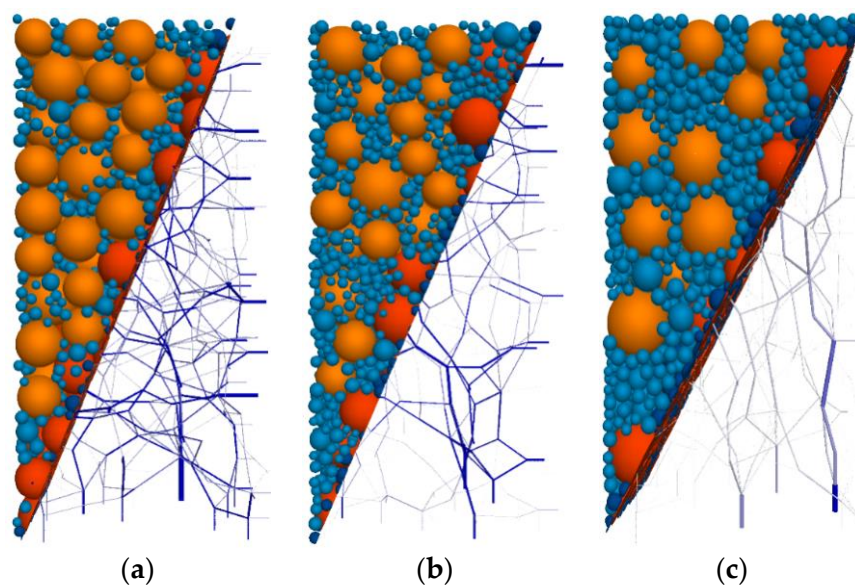


**Figure 11.** Cont.

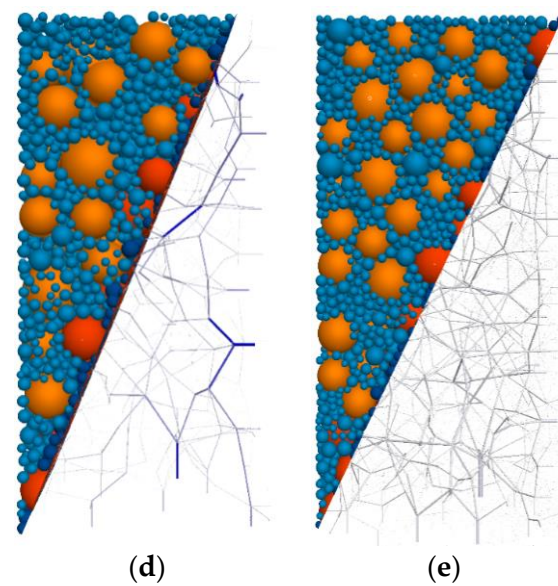


**Figure 11.** Distribution of force chains with different fine grain contents. (a)  $FC = 10\%$  (b)  $FC = 20\%$  (c)  $FC = 30\%$  (d)  $FC = 50\%$  (e)  $FC = 70\%$ .

Vertical force transmission and lateral force transmission are the most common force transmission methods in granular systems. Generally, strong chains mainly transmit force vertically, as shown in Figure 12a. The tree-like structure presented by complex force chain networks is formed due to the transmission path of this force. The force shown in Figure 12b is mainly transmitted horizontally. During horizontal force transmission, the force needs to overcome resistance, such as friction and rotation, causing the force chain in this direction to be generally weak.

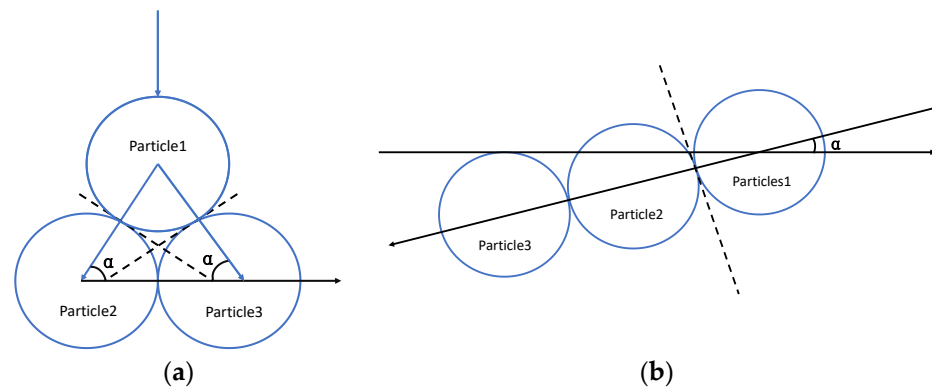


**Figure 12.** Force transmission between grains. (a) Vertical force transmission (b) Horizontal force transmission.

It can be seen from Figure 10 that with the increase of the fine grain content, the fine grain bears more and more force, resulting in a reduction of strong force chains and an increase of weak force chains. The distribution characteristics of the force chain are mainly determined by the stiffness and number of grains. In the consolidation stage, the greater the stiffness and the fewer grains, the higher the strength of the force chain formed, and vice versa. Therefore, in the binary grain structure, coarse grains with higher stiffness tend to form strong chains, and fine grains with lower stiffness tend to form weak chains. With the increase of fine grain content, strong chains are gradually replaced by many weak chains, leading to a change in the structure of force chains. As the weak force chains further grow, the contact between coarse grains no longer exists, and the structure of the strong

force chain is destroyed. In such a case, the force chain distribution is dominated by the weaker ones.

#### 4.3.2. Grain Contact Force Analysis

The micro fabric has an essential influence on the macro mechanical properties of tailings. Rothenburg and Bathurst [48,49] proposed an equation to describe the relationship between the two, which uses the Fourier series to express the distribution functions of the normal contact force and tangential contact force between grains.

$$f_{(n)}(\theta) = f_0 \left[ 1 - a_n \cos 2(\theta - \theta_f) \right] \quad (3)$$

$$f_{(t)}(\theta) = -f_0 a_t \sin 2(\theta - \theta_t) \quad (4)$$

where  $f_{(n)}(\theta)$  and  $f_{(t)}(\theta)$  are the distribution functions of the normal force and tangential force of indirect contact of grains, respectively,  $\theta$  is the angle of contact direction,  $f_0$  is the average normal contact force relative to all contacts,  $\theta_f$  and  $\theta_t$  represent the main directions of normal contact force anisotropy and tangential contact force anisotropy, respectively,  $a_n$  and  $a_t$  are Fourier series coefficients, and their values reflect the degree of anisotropy development of the tailings.

The influence of fine grain content on the structure of tailings can also be quantitatively described through the indirect contact force of grains [50]. Figures 13 and 14 reveal the pattern variation of the initial indirect contact forces of mixed-size grains caused by the change in fine grain content. In Figure 13, the range of  $0^\circ$  to  $330^\circ$  represents the distribution of contact force directions between the tailings grains. Typically, the range of  $90^\circ$  to  $270^\circ$  is defined as the normal direction of grain contact force, while the range of  $0^\circ$  to  $180^\circ$  is considered the tangential direction of grain contact force.

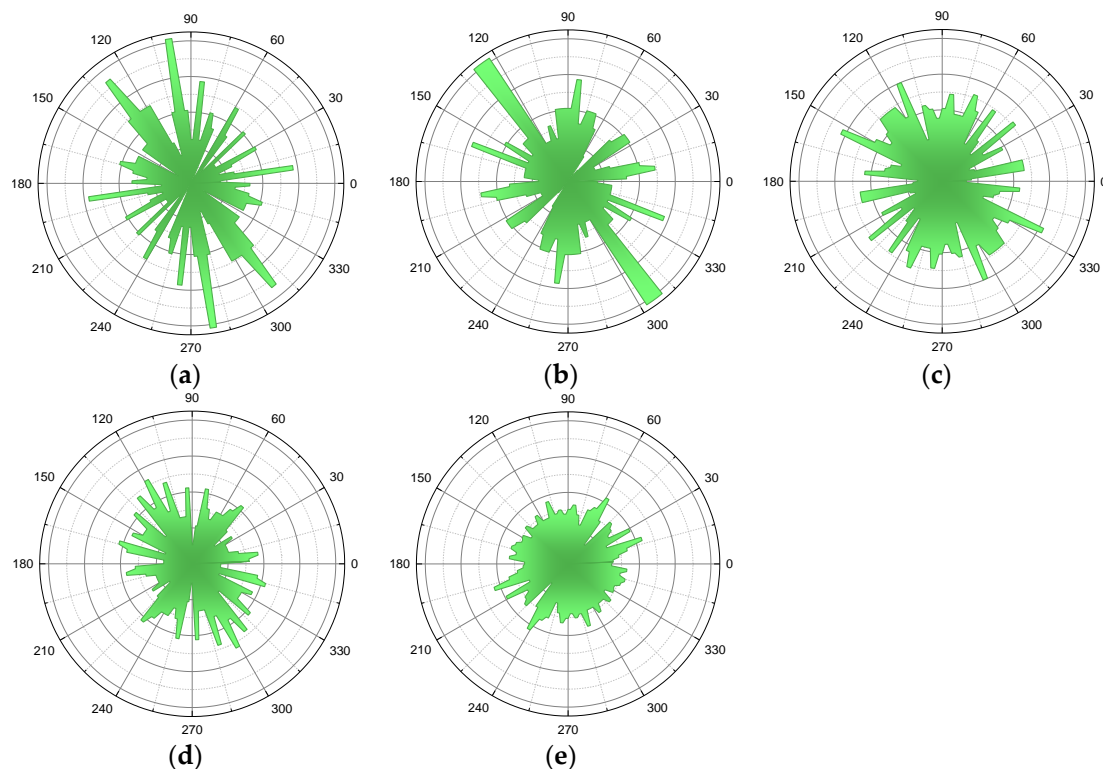


**Figure 13.** Normal contact force between grains with different fine grain contents. (a) FC = 10% (b) FC = 20% (c) FC = 30% (d) FC = 50% (e) FC = 70%.



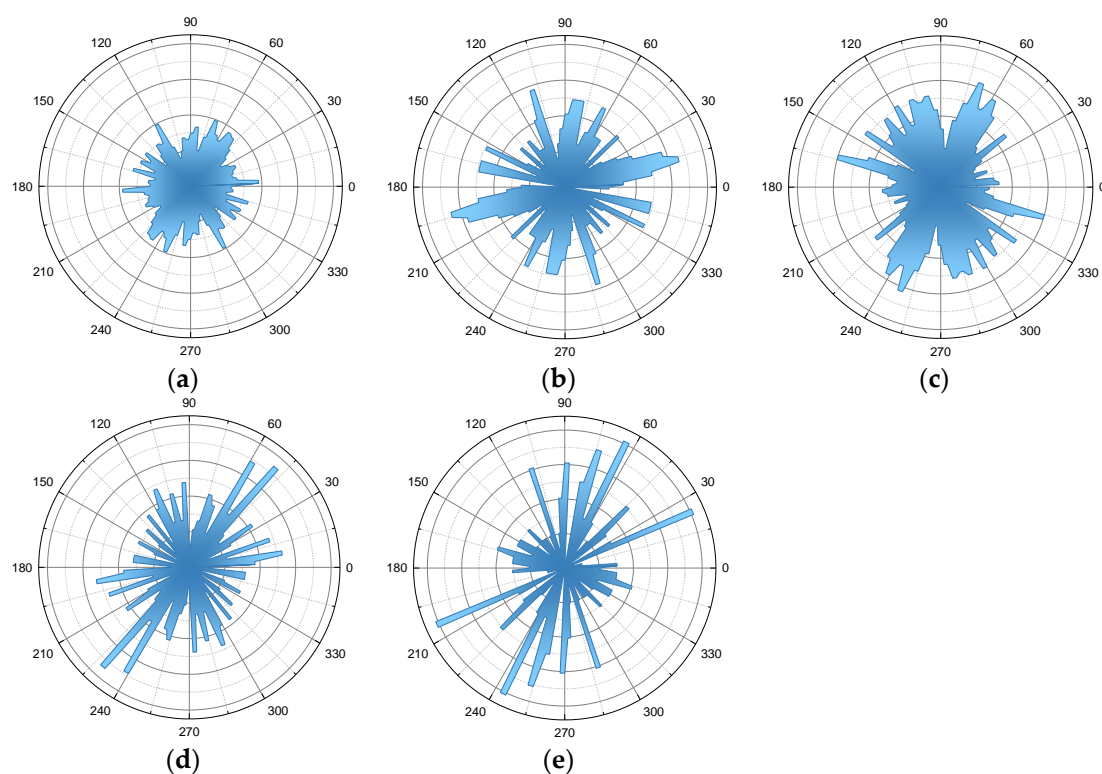


**Figure 14.** Tangential contact force between grains with different fine contents. (a) FC = 10% (b) FC = 20% (c) FC = 30% (d) FC = 50% (e) FC = 70%.

As depicted in the figures, with an increase in the content of fine grains, both the initial normal contact force and the initial tangential contact force decrease. When  $FC < 30\%$  ( $FC = 0\%, 10\%, 20\%$ ), the normal contact force between grains is greater than the tangential contact force, and the mechanical properties of the tailings are mainly determined by the strong chains constructed by coarse grains. When  $FC = 30\%$ , the normal and tangential contact forces are both relatively small and evenly distributed, resulting in the lowest li-quefaction resistance of the tailings. When  $FC > 30\%$  ( $FC = 40\%, 50\%, 60\%, 70\%, 80\%, 90\%, 100\%$ ), the normal contact force is weaker than the tangential contact force, and the mechanical properties of the tailings are mainly determined by the weak force chains constructed by fine grains. Moreover, the normal contact force is mainly distributed in the vertical direction, whereas the tangential contact force is mainly distributed in the horizontal direction, indicating that both of them have undergone a deflection as the content of fine grains increases.

## 5. Discussion

1. In the present work, we classify the tailings into three types, which are coarse-grain tailings, intermediate-grain tailings and fine-grain tailings, by introducing the theory of grain contact states. In total, there are four different grain contact states, which are defined using the fine grain content as a criterion. In the section that discusses the pore pressure development pattern of tailings, we provide an interpretation of the dynamic pore pressure development of tailings from a microscopic perspective. This interpretation takes into account the particle composition and morphology, and is achieved by combining XRD (X-Ray Diffraction) tests with SEM (Scanning Electron Microscope) tests. To analyze the dynamic strength of the tailings, we employed discrete element simulation. This approach enabled us to create a more realistic simulation by generating large and small grains of varying sizes within the model and assigning them different contact types. Subsequently, we analyzed the dynamic

strength of the tailings material using contact force analysis, force chain analysis, and intergranular contact force analysis.

2. In this study, we have examined the fine grain content with a variation of 10%. However, we acknowledge the potential for a more detailed division of the fine grain content, such as  $FC = 28\%$ ,  $FC = 30\%$ ,  $FC = 33\%$ , and so on, which we have not explored extensively in this work. Indeed, this represents the direction of our future research endeavours.
3. The occurrence of earthquakes can induce liquefaction in tailings, potentially resulting in the destabilization and failure of tailings ponds. Currently, the criterion for tailings liquefaction primarily considers a macroscopic perspective. However, it is important to note that the liquefaction phenomenon itself represents a macroscopic manifestation of abrupt changes in the structure of tailings. To comprehend this phenomenon, it is necessary to investigate the dynamic pore pressure and dynamic strength of tailings materials. Notably, substantial variations exist in the dynamic pore pressure and dynamic strength of tailings materials with different fine grain contents. Therefore, studying tailings materials with varying fine grain contents holds significant importance in enhancing our understanding of the phenomenon.

## 6. Conclusions

Investigation of the influence of fine grain content on the mechanical properties of tailings material has significant practical value for tailings engineering. This article studies the microscopic characteristics of tailings material through macro and micro experiments, discrete element simulations, and grain contact state theories, aiming to understand the micromechanical mechanism of tailings with different fine grain contents. The main conclusions are as follows:

- (1) As the fine grain content increases, the grain contact state changes. Based on the theory of grain contact state, tailings with different fine grain contents are divided into coarse grains, intermediate-size grains, and fine grains. When the grains are in contact state 1, the vibration pore pressure exhibits a “fast-stable” development mode with the vibration. When the grains are in contact state 2 or 3, the vibration pore pressure develops linearly with increasing the vibrations. For grains in contact state 4, the development of their vibration pore pressure presents a “fast-stable-sharp” development mode.
- (2) There are significant differences in microscopic observation results between coarse and fine grains. The content of quartz in coarse grains is much higher than that of illite, while the content of quartz in fine grains decreases and the content of illite increases. In terms of grain morphology, all coarse grains exist in granular form, with most of them in edge-to-edge and edge-to-surface contacts. However, the majority of fine grains are sheet-like grains, mainly in edge-to-surface and surface-to-surface contacts.
- (3) The variation in dynamic strength of tailings with different fine grain contents was comprehensively examined by constructing a discrete element simulation model that incorporated various fine grain contents. The dynamic strength was analyzed by investigating the distribution of force chains and inter-grain contact forces. This approach provided a detailed understanding of how the dynamic strength of tailings varies with different fine grain contents.
- (4) With the increase of  $FC$ , the liquefaction resistance of tailings material first decreases and then increases. For the tailings material studied in the present work, its critical threshold of fine grain content ( $FC_{th}$ ) is 30%. When  $FC < 30\%$ , the grain contact is in state 1 or 2, and the liquefaction resistance decreases with the increase of  $FC$ . When  $FC > 30\%$ , the grain contact is in state 3 or 4, and the liquefaction resistance increases with the increase of  $FC$ . The lowest liquefaction resistance occurs when  $FC = 30\%$ .

**Author Contributions:** Methodology, G.W.; Software, Y.Z.; Validation, J.L.; Writing—original draft, C.J. All authors have read and agreed to the published version of the manuscript.

**Funding:** This research was funded by National Natural Science Foundation of China (No. 52174114).

**Conflicts of Interest:** The authors declare no conflict of interest.

## References

1. Qiao, L.; Qu, C.; Cui, M. Analysis of the effect of fines content on the engineering properties of tailings. *Rock Soil Mech.* **2015**, *36*, 923–927+945.
2. Yang, C.; Zhang, C.; Li, Q. Large-scale high tailings dam disaster mechanism and prevention and control methods. *Rock Soil Mech.* **2021**, *42*, 1–17.
3. Seed, H.B.; Tokimatsu, K.; Harder, L.F.; Chung, R.M. The influence of SPT procedures in soil liquefaction resistance evaluations. *J. Geotech. Eng.* **1985**, *111*, 1425–1445. [[CrossRef](#)]
4. Vaid, Y.P.; Fisher, J.M.; Kuerbis, R.H. Grain Gradation and Liquefaction. *Journal Geotech. Eng.* **1990**, *116*, 698–703. [[CrossRef](#)]
5. Amini, F.; Qi, G.Z. Liquefaction testing of stratified silty sands. *J. Geotech. Geoenviron. Eng.* **2000**, *126*, 208–217. [[CrossRef](#)]
6. Monkul, M.M.; Yamamuro, J.A. Influence of silt size and content on liquefaction behavior of sands. *Can. Geotech. J.* **2011**, *48*, 931–942. [[CrossRef](#)]
7. Polito, C.P.; Martin, J.R. A reconciliation of the effects of non-plastic fines on the liquefaction resistance of sands reported in the literature. *Earthq. Spectra* **2003**, *19*, 635–651. [[CrossRef](#)]
8. Xenaki, V.C.; Athanasopoulos, G.A. Liquefaction resistance of sand–silt mixtures: An experimental investigation of the effect of fines. *Soil Dyn. Earthq. Eng.* **2003**, *23*, 1–12. [[CrossRef](#)]
9. Wang, Y.L.; Wang, Y. The Effects of Fines on Post Liquefaction Strength and Deformation Characteristics of Sand. *Adv. Mater. Res.* **2012**, *594–597*, 23–27. [[CrossRef](#)]
10. Vu To-Anh, P.; Hsiao, D.-H.; Phuong Thuc-Lan, N. Critical State Line and State Parameter of Sand-Fines Mixtures. In Proceedings of the International Conference on Sustainable Development of Civil, Urban and Transportation Engineering (CUTE), Ho Chi Minh City, Vietnam, 11–14 April 2016.
11. Lv, X. Experimental Study on the Effect of Fine Particle Content on the Dynamic Properties and Microstructure of Pulverized Soils. Master's Thesis, Zhejiang University of Technology, Hangzhou, China, 2016.
12. Cao, C.; Sun, Y.; Dong, B. Study on the dynamic strength characteristics of powdery soils with different clay particle contents. *Coast. Eng.* **2009**, *28*, 27–32.
13. Liu, X.; Chen, G. Experimental study on the effect of clay particle content on liquefaction of Nanjing fine sand. *Earthq. Eng. Eng. Vib.* **2003**, *3*, 150–155.
14. Zhou, J.; Yang, Y.; Jia, M. Effect of fines content on liquefaction characteristics of saturated sandy soils. *J. Hydraul. Eng.* **2009**, *40*, 1184–1188.
15. Liu, E.; Song, C.; Luo, K. Exploration of dynamic characteristics of coarse-fine grain mixed soil. *World Earthq. Eng.* **2010**, *26* (Suppl. S1), 28–31.
16. Ruan, Y.; Wu, Z. Study of some dynamic properties of saturated powder soils. *Chin. J. Geotech. Eng.* **1995**, *4*, 100–106.
17. El Takch, A.; Sadrekarimi, A.; EL Naggar, H. Cyclic resistance and liquefaction behavior of silt and sandy silt soils. *Soil Dyn. Earthq. Eng.* **2016**, *83*, 98–109. [[CrossRef](#)]
18. Stamatopoulos, C.A. An experimental study of the liquefaction strength of silty sands in terms of the state parameter. *Soil Dyn. Earthq. Eng.* **2010**, *30*, 662–678. [[CrossRef](#)]
19. He, W.; Wang, T. Study of dynamic porosity and related dynamic response characteristics of two-dimensional saturated soils. *Rock Soil Mech.* **2020**, *41*, 2703–2711.
20. Liu, H.; Wang, H.; Zhang, M. Analysis of the dynamic response of the chalky soil seabed in the Yellow River Delta under wave action. *Rock Soil Mech.* **2013**, *34*, 2065–2071.
21. Zhao, C.; Yang, C. Effect of fines content on liquefaction properties of tailings materials. *Rock Soil Mech.* **2006**, *7*, 1133–1137+1142.
22. Zhou, Q.; Xiong, B.; Yang, G. Experimental study on microstructure of low liquid limit powder soil. *Chin. J. Geotech. Eng.* **2013**, *35* (Suppl. S2), 439–444.
23. Zhou, W.; Leng, W.; Liu, W. Study of dynamic properties and backbone curve model of saturated coarse-grained soils under low peritectic cyclic loading. *Rock Soil Mech.* **2016**, *37*, 415–423.
24. Cao, Y.; Wang, T. Experimental study of liquefaction characteristics and pore pressure model of Shanghai chalk soil. *Shanghai Geol.* **1998**, *3*, 60–64.
25. Chen, G.; Liu, X. Study on the development pattern of vibratory pore pressure of powder clay and powder sand interbedded soil and powder fine sand in Nanjing. *Chin. J. Geotech. Eng.* **2004**, *1*, 79–82.
26. Yu, L.; Wang, B. Experimental study of vibratory pore water pressure in saturated powder soils. *J. Dalian Univ.* **1999**, *4*, 59–62.
27. Zhao, X.; Chen, X.; Ding, P. Study of pore pressure development pattern of powder soil with different fine grain content under dynamic load. *J. Wuhan Univ. Technol. (Transp. Sci. Eng.)* **2022**, *46*, 264–269.
28. Zeng, C. Experimental study on the effect of fine particle content on liquefaction characteristics of pulverized soils. *J. Disaster Prev. Mitig. Eng.* **2007**, *4*, 478–483.

29. Zeng, C.; Liu, H.; Chen, Y. Experimental study on the effect of fines content on the development pattern of dynamic pore pressure in powder soils. *Rock Soil Mech.* **2008**, *8*, 2193–2198.
30. Zeng, C.; Liu, H.; Feng, T. Experimental study on pore water pressure properties of saturated powder soil. *Rock Soil Mech.* **2005**, *12*, 1963–1966.
31. Zeng, C.; Liu, H.; Zhou, Y. Experimental study on the development law of dynamic pore pressure influenced by the powder content of saturated powder soil. *J. Disaster Prev. Mitig. Eng.* **2006**, *2*, 180–184.
32. Wang, Y.; Rao, X.; Pan, J. Effect of fine grain content on the evolutionary characteristics of dynamic pore pressure in saturated sandy soils. *Archit. Environ. Eng.* **2011**, *33*, 52–56.
33. Eker, H.; Bascetin, A. Influence of silica fume on mechanical property of cemented paste backfill. *Constr. Build. Mater.* **2022**, *317*, 126089. [[CrossRef](#)]
34. Bi, Q.; Li, C.-h.; Chen, J.-x. Effect of fine particle content on mechanical properties of tailings under high confining pressure. *Arab. J. Geosci.* **2021**, *14*, 942. [[CrossRef](#)]
35. Adiguzel, D.; Bascetin, A. The investigation of effect of particle size distribution on flow behavior of paste tailings. *J. Environ. Manag.* **2019**, *243*, 393–401. [[CrossRef](#)]
36. Wang, Y.; Wang, Y. Study on the influence of fine particle content on dynamic elastic modulus and damping ratio of saturated sand. *Rock Soil Mech.* **2011**, *32*, 2623–2628. [[CrossRef](#)]
37. Cui, M.; Zheng, J.; Lai, H. Experimental study on the effect of particle size on the strength of microbial solidified sand. *Rock Soil Mech.* **2016**, *37* (Suppl. S2), 397–402. [[CrossRef](#)]
38. Thevanayagam, S.; Mohan, S. Intergranular state variables and stress-strain behaviour of silty sands. *Geotechnique* **2000**, *50*, 1–23. [[CrossRef](#)]
39. *Geotechnical Test Procedures: GBT 50123-2019*; General Institute of Water Resources and Hydropower Planning and Design, Ministry of Water Resources, Nanjing Institute of Water Resources Science. China Planning Press: Beijing, China, 2019.
40. Gao, Y.; Yu, Z.; Chen, W.; Yin, Q.; Wu, J.; Wang, W. Recognition of rock materials after high-temperature deterioration based on SEM images via deep learning. *J. Mater. Res. Technol. J. Mater. Res. Technol.* **2023**, *25*, 273–284. [[CrossRef](#)]
41. Wang, T.; Zhu, J.; Liu, S. Discrete element simulation of plastic behavior of soil and rock mixes with different fines content. *Chin. J. Theor. Appl. Mech.* **2022**, *54*, 1075–1084.
42. Gong, B.; Jiang, Y.; Chen, L. Feasibility investigation of the mechanical behavior of methane hydrate-bearing specimens using the multiple failure method. *J. Nat. Gas Sci. Eng.* **2019**, *69*, 102915. [[CrossRef](#)]
43. Guo, Y.; Peng, Z.; Tian, Y. Numerical simulation of particle flow in triaxial compression of a metal mine tailings. *Min. Res. Dev.* **2021**, *41*, 118–123.
44. Gong, B.; Jiang, Y.; Yan, P.; Zhang, S. Discrete element numerical simulation of mechanical properties of methane hydrate-bearing specimen considering deposit angles. *J. Nat. Gas Sci. Eng.* **2020**, *76*, 103182. [[CrossRef](#)]
45. Wu, S.; Yang, C.; Zhang, C. Effect of powder content on mechanical properties of tailings. *Chin. J. Geotech. Eng.* **2017**, *36*, 2007–2017.
46. Liu, J.; Wautier, A.; Bonelli, S.; Nicot, F.; Darve, F. Macroscopic softening in granular materials from a mesoscale perspective. *Int. J. Solids Struct.* **2020**, *193–194*, 222–238. [[CrossRef](#)]
47. Wang, X.; Zhang, S.; Zhao, K. Experimental and analytical model of the effect of fine-grained soil content on the salt swelling characteristics of coarse-grained sulfate saline soil roadbed fill. *Rock Soil Mech.* **2022**, *43*, 2191–2202.
48. Kruyt, N.P.; Rothenburg, L. Statistics of the elastic behaviour of granular materials. *Int. J. Solids Struct.* **2001**, *38*, 4879–4899. [[CrossRef](#)]
49. Rothenburg, L.; Bathurst, R.J. Analytical study of induced anisotropy in idealized granular materials. *Geotechnique* **1989**, *39*, 601–614. [[CrossRef](#)]
50. Liu, Y.; Wu, S.; Zhou, J. Numerical simulation of sandy soil deformation process under monotonic load and study of fine view mechanism. *Rock Soil Mech.* **2008**, *29*, 3199–3204+3216. [[CrossRef](#)]

**Disclaimer/Publisher's Note:** The statements, opinions and data contained in all publications are solely those of the individual author(s) and contributor(s) and not of MDPI and/or the editor(s). MDPI and/or the editor(s) disclaim responsibility for any injury to people or property resulting from any ideas, methods, instructions or products referred to in the content.